

# Phase-Field Simulation of Microsegregation and Dendritic Growth During Solidification of Hypoeutectic Al-Cu alloys

Alexandre Furtado Ferreira<sup>a\*</sup>, Késsia Gomes Paradela<sup>a</sup>, Paulo Felipe Junior<sup>a</sup>, Zilmar Alcântara Júnior<sup>a</sup>, Amauri Garcia<sup>b</sup>

<sup>a</sup> Graduate Program on Metallurgical Engineering, Federal Fluminense University, 27255-125, Volta Redonda, RJ, Brazil

<sup>b</sup> Department of Manufacturing and Materials Engineering, University of Campinas - UNICAMP, 13083-860, Campinas, SP, Brazil

Received: March 03, 2016; Revised: December 14, 2016; Accepted: January 03, 2017.

Prediction of microstructure evolution and microsegregation is one of the most important problems in materials science. The dendritic growth and microsegregation provide a challenging simulation goal for computational models of solidification, in addition to being an important technological feature of many casting processes. The phase-field model offers the prospect of being able to perform realistic simulation experiments on dendrite growth in metallic systems. In this paper, the microsegregation and dendritic growth of hypoeutectic Al-Cu alloys under constant cooling rate was simulated using a phase-field model. The main new feature of the present model is based on the fact that the effect of the growth rate is incorporated via an effective partition coefficient that has been experimentally determined for a range of growth rates. It is shown that both models (Phase-field model and Scheil) have significant deviations from the experimental data when the equilibrium partition coefficient is considered in the calculations. Since the predicted results using the models yielded discrepancies from the experimental data, an experimental equation is adopted for calculating the effective partition coefficient from experimental data. The experimental equation is then adopted in the calculations of phase-field model and Scheil's equation, showing a good agreement with the experimental data.

**Keywords:** Alloys; Solidification; Microstructure; Computer modelling and simulation

## 1. Introduction

Solidification processing is one of the important routes to produce metallic materials, especially alloys. The conditions for the solidification process, such as the temperature gradient and the growth rate, vary from process to process and in one process also as a function of time and space. These variations together with the different alloy compositions, lead to a multitude of microstructures and therefore material properties. Since the properties of an alloy can depend strongly on the concentration of solutes that it contains, being able to quantitatively predict the concentrations in the solid is desirable. One important phenomenon, which has to be well controlled, is the so-called segregation. The solidification leads to types of segregation; micro and macro segregation. Microsegregation; which occurs over short distances comparable to the dendrite arm spacing. The macrosegregation, in turn, occurs over similar distances to the size of the casting.

Over the last 10 years the phase-field model has been used for simulations of the solidification process. The phase-field model is known to be a computational tool for describing the pattern evolution of the interface between

mother and new phases in non-equilibrium state because all the governing equations are written in a unified manner in the whole space of the system. The order parameter takes on constant values in the solid region and liquid and changes steeply but smoothly over a thin transition layer that plays the role of the classical sharp interface. The governing equations coupled with modified transport equation are applied in the whole computational domain without distinguishing between the phases. This permits simulations of dendritic evolutions without explicitly tracking the interface.

The solidification process of alloys has been studied by Salvino et al.<sup>1,2</sup> It is shown, in said work, the phase-field model applied to the multicomponent alloy solidification (Fe-C-P-Mn) for equiaxed dendritic growth. The papers provide an introduction to the phase-field model and an overview of its possibilities. Amongst the possible applications, in these papers, the phase-field model is applied to estimate the solidified fraction during sundry examples of solidification processes. Microsegregation behavior in multicomponent alloys is analyzed and compared with analytical models. The solid concentration profiles in solid/liquid interface calculated by the phase-field model show good agreement with those

\* e-mail: [furtado@metal.eeimvr.uff.br](mailto:furtado@metal.eeimvr.uff.br)

from the Clyne–Kurz equation. Such good agreement is due to back-diffusion of solute into the solid phase from the solid/liquid interface, which is taken into account in the Clyne–Kurz equation. Liu et al.<sup>3</sup> used the phase-field model to the simulation of equiaxed dendritic growth under convection. The influence of flow on the dendrite morphology and the concentration was investigated during the alloy solidification; the microsegregation was studied by changing the forced flow velocity. The results showed that upstream dendritic arm is promoted with convection, while the downstream is inhibited, and the perpendicular arms grow towards to upstream direction. Li et al.<sup>4</sup> studied the microsegregation during solidification of a binary alloy by phase-field simulations. The microsegregation within the columnar dendritic array is analyzed by performing a two-dimensional phase-field simulation. The influence of microstructure morphology on microsegregation was studied for various back diffusion conditions. Under the condition of no back diffusion, it is found that at the region without second dendrite arms the simulation result agrees well with Scheil's equation, but for the region with well developed secondary dendrite arms there is a severe deviation. This deviation, according to Li et al.<sup>4</sup>, is attributed to the dendritic coarsening and the inhomogeneity of interdendritic liquid concentration caused by various interface curvatures. Under the condition of moderate back diffusion, it is found that the effect of dendritic morphology on microsegregation can be accounted by enhancing the Fourier number, which characterizes the solid-state diffusion. A modelling approach is presented by Warnken et al.<sup>5</sup>, for the prediction of microstructure evolution during directional solidification of nickel-based superalloys, using a phase-field model. The phase-field model was coupled to CALPHAD thermodynamic and kinetic databases, for solidification simulation in multicomponent system. The dendritic growth and the formation of interdendritic phases in an isothermal region are simulated for a range of solidification parameters. It is demonstrated that the predicted patterns of microsegregation obtained from the simulations compare well to the experimental results. Recently, Wei et al.<sup>6</sup> performed a computational study of the equiaxed microstructure and microsegregation in an industrial A2214 alloy during solidification by means of two-dimensional domain with phase-field model. The microstructure simulated by phase-field model reproduces the experimental data very well. This indicates that a quantitative phase-field simulation can be achieved with good results. Moreover, the mechanisms of characteristic patterns and microstructure formation were revealed with the aid of the phase-field simulation. The effect of cooling rate on the secondary dendrite arm spacing and microsegregation was investigated through comparison with the experimental results. The previous works<sup>1-6</sup> indicate that the phase-field model is a versatile and powerful technique for calculating the evolution of microstructure, which is very popular nowadays.

The model was originally proposed to simulate solidification of pure materials<sup>7-9</sup> and has been extended to solidification of alloys<sup>10-14,16-18</sup>. In contrast to the previous phase-field models, in the present paper the numerical results are achieved in the simulations by disregarding the equilibrium partition coefficient ( $K_e$ ) and, instead, imposing an effective partition coefficient ( $K_{eff}$ ). This difference constitutes the main new feature of the present model. The directional solidification of a hypoeutectic Al-Cu alloy under unsteady-state thermal conditions is simulated by the proposed phase-field model. The aluminium alloys (Al-CU) have been chosen taking into account their high strength, which is achieved by the heat treatment process, furthermore, the cast aluminium alloys yield cost-effective products due to the low melting point. In this present paper, the phase-field model is applied in solidification of two binary alloys Al- $2.64 \times 10^{-2}$  mol%Cu (6.0wt.%Cu) and Al- $4.5 \times 10^{-2}$  mol%Cu (8.9wt.%Cu). The microsegregation level can be affected by the formation of eutectic phase during the solidification process in Al-Cu alloys. The formation of eutectic phase in the solidification, in turn, is strongly affected by copper concentration in aluminium alloys. Results obtained by Kurum et al.<sup>22</sup> point out that eutectic phase will form according to the increasing of copper concentration, experimental data of aluminium alloy with high copper concentration ( $4.5 \times 10^{-2}$  mol%Cu) showed the eutectic phase formed in the final stage of solidification process. The motivation of choosing copper composition ( $2.64 \times 10^{-2}$  and  $4.5 \times 10^{-2}$  mol%Cu), it is due in this compositions and range of solid fraction (0 to 80%), the solidification occurs without intermetallic phase and eutectic formation. The solidification experiments carried out by Meza et al.<sup>15</sup> are briefly discussed to follow: In said experiments, hypoeutectic Al–Cu alloys were directionally solidified under unsteady-state heat flow conditions in a water-cooled solidification setup. The experimental cooling curves allowed solidification thermal parameters: cooling rate and growth rate to be experimentally determined and correlated with the scale of the dendritic (Al–Cu alloys) patterns. Experimental microsegregation profiles from the central part of the dendrite cores to the limit of the interdendritic regions were determined by Meza et al.<sup>15</sup> in the different growth rates. For simplicity, in this present paper, it is assumed that said alloys are diluted; therefore the copper is completely soluble in the aluminium. The effect of the growth rate was incorporated into an effective partition coefficient that has been determined for the range of growth rates experimentally examined. The microsegregation profiles predicted by both the phase-field model and Scheil's equation, using the new partition coefficient, are compared with experimental data.

## 2. Governing Equations

The phase-field model is a mathematical model for solving interface problems. For the solidification case,

there are three distinct regions to consider: solid, liquid and interface. The interface in this mathematical description is a two-dimensional surface with width defined. In the phase-field model, the state of the computational domain is represented continuously by order parameter ( $\phi$ ). For example,  $\phi = +1$ ,  $\phi = 0$  and  $0 < \phi < +1$  represent the solid, liquid and interface respectively. The latter is therefore located by the region over which  $\phi$  changes from liquid-value to its solid-value. The range over which the order parameter changes is the width of the interface. The set of values of the order parameter over the whole computational domain is the phase field. The evolution of the solid region with time is assumed to be proportional to the variation of the free energy functional with respect to the order parameter. So, in this present paper, the phase-field model is briefly summarized, readers can refer to literatures<sup>19-20</sup> for more details of the formulation. For simulation of microstructures in binary alloys during solidification, we used two equations: one for solute concentrations, the other for the phase field itself. Following Ferreira et al.<sup>11</sup>, the first equation takes the form

$$\frac{1}{M} \frac{\partial \phi}{\partial t} = \varepsilon^2 \nabla^2 \phi - Wg'(\phi) + \frac{RT}{V_m} h'(\phi) \ln \left[ \frac{(1 - c_S^e)(1 - c_L)}{(1 - c_L^e)(1 - c_S)} \right] \quad (1)$$

where “ $\ln$ ” stands for the principal argument of the natural logarithm of the fraction function within the square brackets and the respective ordinary concentrations in the liquid and solid region are denoted, by pair,  $C_L$  and  $C_S$ . As for the phase-field equation, those authors propose

$$\frac{\partial c}{\partial t} = \nabla \left\{ \frac{D(\phi) [(1 - h(\phi))(1 - c_L)c_L + h(\phi)(1 - c_S)c_S]}{h(\phi)(1 - c_S)c_S} \nabla \ln \left( \frac{c_L}{1 - c_L} \right) \right\} \quad (2)$$

where  $h(\phi) = \phi^2(3 - 2\phi)$ ,  $g(\phi) = \phi^2(1 - \phi)^2$ , and the subscripts  $S$  and  $L$  stand for solid and liquid, respectively.  $M$  and  $\varepsilon$  are phase-field parameters;  $D(\phi)$  is the solute diffusion coefficient. These phase-field parameters are related to the interface energy,  $\sigma$ , whereas the interface width,  $2\lambda$ , is the distance over which  $\phi$  changes from 0.1 to 0.9. Notice, furthermore, that  $M$  is also related to the kinetic coefficient,  $\beta$ , defined to be the inverse of the usual linear kinetic coefficient,  $\mu_k$ . From Salvino et al.<sup>1</sup>, these are obtained as

$$\sigma = \frac{\varepsilon_0 \sqrt{W}}{3\sqrt{2}} \quad (3)$$

$$2\lambda = 2.2\sqrt{2} \frac{\varepsilon_0}{\sqrt{W}} \quad (4)$$

$$\beta = \left( \frac{V_m}{RT} \right) \left( \frac{\sigma}{\varepsilon^2 M} - \frac{\varepsilon_0}{D_i \sqrt{2W}} \xi(c_S^e, c_L^e) \right) \frac{m_e}{1 - K_{ef}} \quad (5)$$

$$\xi(c_S^e, c_L^e) = \frac{RT}{V_m} (c_L^e - c_S^e)^2 \times \int_0^1 \frac{(1 - h(\phi))h(\phi)}{(1 - h(\phi))(1 - c_L^e)c_L^e + h(\phi)(1 - c_S^e)c_S^e} \frac{d\phi}{(1 - \phi)\phi} \quad (6)$$

where  $m_e$  is the slope of the liquidus line at equilibrium,  $K_{ef}$  is the effective partition coefficient, and  $D_i$  is the diffusion coefficient in the interface region. For the binary-alloy system, we use the same parameters shown in the literature, Ferreira et al.<sup>16</sup> In addition,  $T$  is the temperature,  $W$  represents the interface energy, and  $V_m$  is the molar volume. — Equations (1) and (2) were solved numerically. They were discretized on uniform grids using an explicit finite scheme.

Anisotropy is introduced in the phase-field model as follows:

$$\varepsilon(\theta) = \varepsilon_0 \{1 + \delta_\varepsilon \cos(j \cdot (\theta - \theta_0))\} \quad (7)$$

where  $\delta_\varepsilon$  gauges the anisotropy. The value  $j$  controls the number of preferential growth directions. For example, with  $j=0$ , we shall be looking at a perfectly isotropic case, while  $j=4$  is indicative of a dendrite with four preferential growth directions. Orientation of the maximum-anisotropy interface is identified by the  $\theta_0$  constant of Eq. (7),  $\theta$  being the angle between the direction of the phase-field gradient and the reference axis of the system.

### 3. Results and discussion

The parameters used in the phase-field model, obtained from physical properties of the material, were derived from Equation (3) to (6). The boundary condition adopted for the phase-field model ( $\phi$ ) in this work is a zero-flux condition. The governing equations, (1) and (2) above, are solved numerically, using a finite-difference scheme. In the calculations, the system temperature is uniform and continuously decreased with a constant cooling rate from the initial temperature ( $T_0$ ), which is slightly lower than the liquidus temperature of the Al-Cu alloy. The physical properties of binary alloy that were used to simulation are presented in Table 1.

Simulations are carried out disregarding the energy equation and instead imposing the following linear temperature profile:

$$T = T_0 - \dot{T}t \quad (8)$$

where  $T_0$  is the initial temperature,  $\dot{T}$  represents a constant value for the cooling rate and  $t$  is the solidification time. Figure 1 exhibit the measured microsegregation profiles and predicted for a binary alloy Al-Cu. In that figure, one can see that the copper concentration increases with the solid fraction. The experiments were performed with Al-Cu alloys under unsteady state of solidification, thus the Scheil's equation was chosen to describe solute concentration in the solid region. We compare the experimental results<sup>15</sup> with the predictions of a one-dimensional phase-field calculation and by the Scheil's equation. In the both cases, we used in the

**Table 1:** Physical properties of the binary alloy (Al-Cu).

Melting temperature of the pure aluminium, <sup>16</sup> $T_m$ [K]	933.0
Diffusivity in liquid phase, <sup>15</sup> $D_L$ [ $m^2s^{-1}$ ]	$3.6 \times 10^{-9}$
Diffusivity in solid phase, <sup>16,18</sup> $D_S$ [ $m^2s^{-1}$ ]	$3.0 \times 10^{-13}$
Equilibrium partition coefficient, <sup>15</sup> $K_e$	0.1004
Slope of liquids line, <sup>16</sup> $m_c$ [ $Kmol^{-1}$ ]	640
Molar volume, <sup>16</sup> $V_m$ [ $m^3mol^{-1}$ ]	$1.095 \times 10^{-5}$
Interface energy, <sup>21</sup> $\sigma$ [ $Jm^{-2}$ ]	0.093
linear kinetic coefficient, <sup>16</sup> $\mu_k$ [ $mK^{-1}s^{-1}$ ]	0.4

calculations, the equilibrium partition coefficient ( $K_e$ ). The simulation results of the phase-field model show reasonable agreement with those from the Scheil's equation. However, the phase-field model is able to calculate the back-diffusion. Instead, Scheil's analytical model neglected diffusion in the solid phase altogether, but assumed complete mixing of the solute in the liquid phase. One can see that both the predicted and experimental results for the microsegregation profiles differ considerably, this occurs because the equilibrium partition coefficient ( $K_e$ ) is assumed to calculate the solute concentration during solidification process. Interestingly, one of the rapid solidification effects is significant deviations from the equilibrium phase diagram. In this paper, the rapid solidification effects of the solidification process were incorporated through the growth rate into an effective partition coefficient ( $K_{ef}$ ), as proposed by Meza et al.<sup>15</sup>

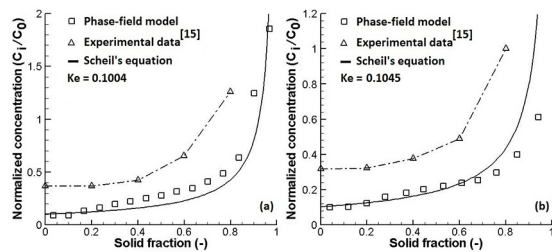
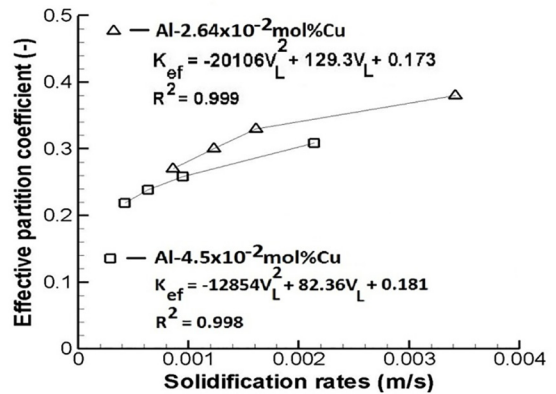
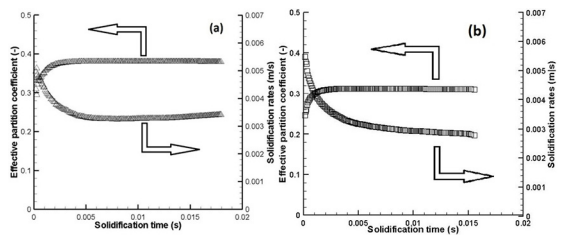
**Figure 1:** Comparison between experimental microsegregation profiles and predicted by the Scheil's equation and phase-field model: (a) Al- $2.64 \times 10^{-2}$  mol%Cu with  $K_e = 0.1004$  and (b) Al- $4.5 \times 10^{-2}$  mol%Cu with  $K_e = 0.1045$ .

Figure 2 shows the experimental data of the effective partition coefficient ( $K_{ef}$ ) as a function of solidification rates ( $V_L$ ).

From the data obtained by Meza et al.<sup>15</sup>, we proposed experimental equations for the partition coefficient as a function of the solidification rate, as showed in Figure 2. The effective partition coefficient ( $K_{ef}$ ) increases with the solidification rate; in the other words the growth rate has a significant role on the partition coefficient. The origin of such changes of the partition coefficient is closely linked solidification kinetics, in the other words; the increasing of solidification speed favors the departure from equilibrium. These experimental equations for the effective partition coefficient ( $K_{ef}$ ) of the Al-Cu alloys are considered in the

**Figure 2:** Effective partition coefficient ( $K_{ef}$ ) versus solidification rates ( $V_L$ ).

phase-field model by equation 5. Figures 3a-b correlates the solidification rate ( $V_L$ ) and the effective partition coefficient ( $K_{ef}$ ) with time during the solidification process for the Al- $2.64 \times 10^{-2}$  mol%Cu and Al- $4.5 \times 10^{-2}$  mol%Cu alloys. As depicted in Figures 3a-b, both the partition coefficient and the solidification rate vary significantly with time immediately after the onset of solidification, followed by essentially constant values.

**Figure 3:** Effective partition coefficient ( $K_{ef}$ ) and solidification rates ( $V_L$ ) versus solidification time ( $t$ ): (a) Al- $2.64 \times 10^{-2}$  mol%Cu and (b) Al- $4.5 \times 10^{-2}$  mol%Cu alloys.

Figures 4a-b displays results obtained with a two-dimensional simulation of an Al-Cu dendrite for two different copper concentrations with solidification time equal to 0.002 s. In this simulation non-isothermal dendrite growth and the effective partition coefficient ( $K_{ef}$ ) were assumed. In order to analyze the effect of initial copper concentration on the dendrite morphology, simulations were carried out, separately. An approach was used, in which a solid nucleus is previously added at the center of the computational domain. The preferential growth angle ( $\theta_0$ ) of the dendrite tip with respect to the x axis is  $45^\circ$ . The anisotropy mode is  $j = 4$ . The concentration field during solidification process is depicted in Figures 4a-b. In the picture, the gray scale represents solute concentration, while the white contour represents the concentration of the copper segregated from the solid to the liquid region. The copper concentration in the solid region is much less than that in the liquid. In Figure 4a, one can see that many secondary arms emerge

and grow up while the primary arms grow, and the secondary arms try to grow upright to the primary arms. Because of the solute redistribution, it can be seen that interdendritic concentration is high, and the primary arms spine, as well as the secondary arms spine are relatively low. Figure 4b shows the results of simulation for the Al-4.5×10<sup>-2</sup>mol%Cu alloy. It depicts the effect of changes on the initial concentration of the system. From the contrast between Figures 4a and 4b, it can be seen that the dendritic morphologies are evidently different. First of all, the primary and secondary arms are much longer and thicker; second, one can see that the field of segregated solute is thinner, Figure 4a. The secondary arms are not well developed with an additional copper concentration, because of copper enrichment at the interface and reduction of interface mobility, Figure 4b. In other words, by increasing the alloy copper concentration, the dendrites become narrower.

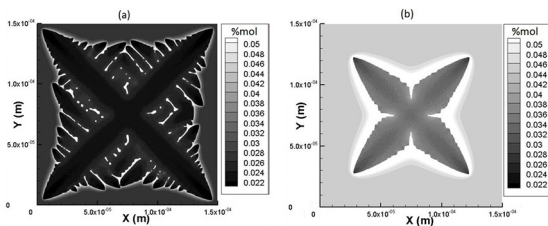


**Figure 4:** Dendrites calculated by the phase-field model for different initial concentrations ( $C_0$ ) of copper, Al-2.64×10<sup>-2</sup>mol%Cu (a) and Al-4.5×10<sup>-2</sup>mol%Cu (b).

The phase-field mobility ( $M$ ) is calculated by equation 5, during simulation of solidification. The results of phase-field mobility for each binary alloy (Al-2.64×10<sup>-2</sup>mol%Cu and Al-4.5×10<sup>-2</sup>mol%Cu), it is showed in Figure 5. There, the solid/liquid interface velocity decreases, depending on the initial concentration ( $C_0$ ), due to a variation in phase-field mobility ( $M$ ) as just mentioned.

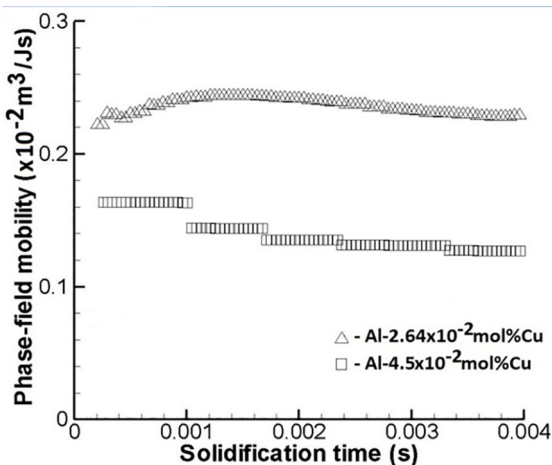


**Figure 5:** Phase-field mobility versus solidification time for the Al-2.64×10<sup>-2</sup>mol%Cu and Al-4.5×10<sup>-2</sup>mol%Cu alloys.

The change in the phase-field mobility ( $M$ ) is inversely proportional to the initial concentration ( $C_0$ ), Figure 5. These results show that a change in initial concentration ( $C_0$ ) affects both the dendrite morphology significantly (Figure 4) and the phase-field mobility (Figure 5). Figure 6 shows new predicted microsegregation profiles, in which the effective partition coefficient ( $K_{ef}$ ) has been adopted, while the experimental data are the same from Figure 2. For all the predicted results in Figure 6, the simulation plot is shifted up, improving the predictions. This is so because the effect of the growth rate has been included on the effective partition coefficient ( $K_{ef}$ ), both in the phase-field model and Scheil's equation. This difference constitutes the main new feature in the phase-field model. A more elaborate microstructure model would allow improvements to the prediction of the solute concentration to be attained, providing some microstructural information that might be of great interest for materials processing. That would be possible, if the present model could incorporate the real properties of the rapid solidification process. The difficulty arises from the fact that an experimental apparatus would be necessary allowing solidification thermal parameters such as the cooling rate and the growth rate to be experimentally determined and correlated with the scale of the dendritic microstructure.

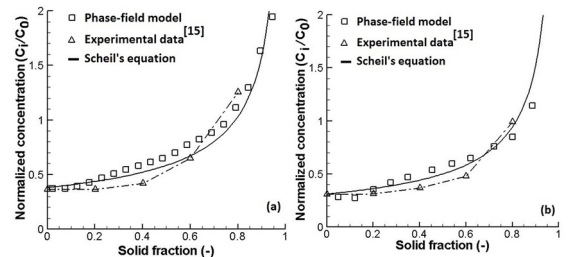


**Figure 6:** Comparison between experimental microsegregation profiles and predictions furnished by Scheil's equation and the phase-field model with  $K_{ef}$ : (a) Al-2.64×10<sup>-2</sup>mol%Cu and (b) Al-4.5×10<sup>-2</sup>mol%Cu alloys.

Figure 7 shows the microsegregation ratio for the two cases examined in the present study: Al-2.64×10<sup>-2</sup>mol%Cu and Al-4.5×10<sup>-2</sup>mol%Cu alloys. The microsegregation ratio is given by the ratio of the maximum concentration (maximum interdendritic concentration) in the liquid region and the initial alloy concentration ( $C_0$ ). The microsegregation ratio of the binary alloy with the initial concentration equal to 2.64×10<sup>-2</sup>mol% is higher than that of the alloy having an initial concentration of 4.5×10<sup>-2</sup>mol%. The reason is that the driving force is larger for the phase transformation of the Al-2.64×10<sup>-2</sup>mol%Cu alloy. The driving force behind the solidification process is quantified by the last product on the right-hand side of equation 1. From Figure 7, it can be seen by comparing the results of both alloys that the variation of the microsegregation ratio has a similar profile. In that figure, the microsegregation ratio is seen to increase faster

at the onset of solidification. This is because  $C_{max}$  increases quickly due to the copper enrichment ahead of the growth interface, at the beginning of solidification. However,  $C_{max}$  changes slightly in the remaining time, when the thickness of the diffusion boundary layer in the liquid region becomes steady. For this reason, the rate then gradually dwindles toward to a constant value.

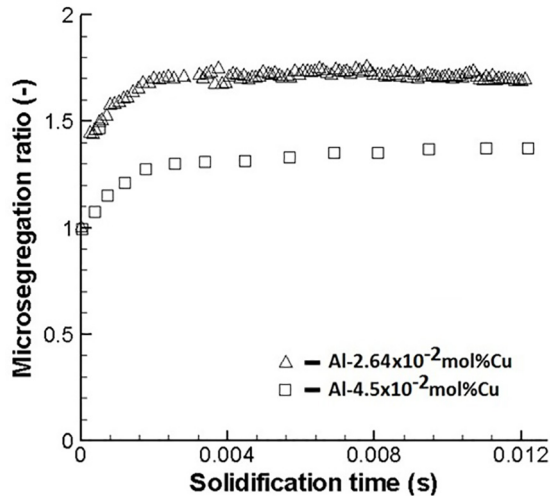


**Figure 7:** The microsegregation ratio ( $C_{max}/C_0$ ) versus solidification time ( $t$ ).

#### 4. Conclusions

Despite the tremendous effort and developments in solidification modeling applications, there still remains a comprehensive demand for further understanding of the physical mechanisms behind microstructural formation, involving the effects of processing conditions on the microstructure and microsegregation of alloys used in technical applications.

By performing comparisons between experimental microsegregation profiles and theoretical ones predicted by Scheil's equation and the phase-field model (both models with equilibrium partition coefficient), it was found that the computed results showed reasonable agreement between them. However, the calculated and experimental results differ considerably. This has been attributed to the use of equilibrium partition coefficients in the calculations, since rapid solidification effects led to significant deviations from the equilibrium phase diagram. In contrast to the previous phase-field models, in the present study the numerically simulated results were obtained by incorporating the effect of the growth rate into effective partition coefficients, which had been experimentally determined for a range of growth rates. It was shown that such approach has led to good agreement between measured and predicted microsegregation profiles of Al-2.64×10<sup>-2</sup>mol%Cu and Al-4.5×10<sup>-2</sup>mol%Cu alloys. In order to analyze the effect of copper concentration on the morphology of the resulting dendrites, two-dimensional simulations were carried out, separately, for Al-2.64×10<sup>-2</sup>mol%Cu

and Al-4.5×10<sup>-2</sup>mol%Cu alloys. It was shown that with the increase in copper concentration, the dendrite becomes narrower and the secondary arms are not well developed, and that was caused by solute enrichment at the growth interface and reduction in interface mobility. The microsegregation ratio was shown to be higher for the alloy having the lowest solute concentration. This has been attributed to the higher solidification driving force associated with the alloy of initial concentration equal to 2.64×10<sup>-2</sup>mol%. Since the growth is faster, therefore, there is less time for diffusion of copper in the liquid region, thus provoking an increase in the concentration of the interdendritic liquid.

#### 5. References

1. Salvino IM, Ferreira LO, Ferreira AF. Simulation of Microsegregation in Multicomponent Alloys During Solidification. *Steel Research International*. 2012;83(8):723-732.
2. Salvino IM, Jácome PAD, Ferreira AF, Ferreira IL. An analysis of the Physical Properties of Multicomponent Alloys on the Simulation Solidification by Phase-Field Model. *Materials Science Forum*. 2013;730-732:703-708.
3. Liu MX, Wang K, Xia D, Jiang T. Phase-field simulation of Al-Si binary dendritic growth and micro-segregation patterns under convection. *Journal of Alloys and Compounds*. 2014;589:431-435.
4. Li J, Wang J, Yang G. Investigation into microsegregation during solidification of a binary alloy by phase-field simulations. *Journal of Crystal Growth*. 2009;311(4):1217-1222.
5. Warnken N, Ma D, Drevermann A, Reed RC, Fries SG, Steinbach I. Phase-field modelling of as-cast microstructure evolution in nickel-based superalloys. *Acta Materialia*. 2009;57(19):5862-5875.
6. Wei M, Tang Y, Zhang L, Sun W, Du Y. Phase-Field Simulation of Microstructure Evolution in Industrial A2214 Alloy During Solidification. *Metallurgical and Materials Transactions A*. 2015;46(7):3182-3191.
7. Ferreira AF, Ferreira LO, Assis AC. Numerical simulation of the solidification of pure melt by a phase-field model using an adaptive computation domain. *Journal of the Brazilian Society of Mechanical Sciences and Engineering*. 2011;33(2):125-130.
8. Kobayashi R. Modeling and numerical simulations of dendritic crystal growth. *Physica D: Nonlinear Phenomena*. 1993;63(3-4):410-423.
9. Kim SG, Kim WT, Lee JS, Ode M, Suzuki T. Large Scale Simulation of Dendritic Growth in Pure Undercooled Melt by Phase-Field Model. *ISIJ International*. 1999;39(4):335-340.
10. Warren JA, Boettinger WJ. Prediction of dendritic growth and microsegregation patterns in a binary alloy using the phase-field method. *Acta Metallurgica et Materialia*. 1995;43(2):689-703.
11. Ferreira AF, de Melo EG, Ferreira LO. Prediction of Secondary-Dendrite Arm Spacing for Binary Alloys by Means of a Phase-Field Model. *Steel Research International*. 2015;86(1):58-64.
12. Ferreira AF, Castro JA, Ferreira IL. 2D Phase-Field Simulation of the Directional Solidification Process. *Applied Mechanics and Materials*. 2015;704:17-21.
13. Ode M, Suzuki T. Numerical Simulation of Initial Microstructure Evolution of Fe-C Alloys Using a Phase-field Model. *ISIJ International*. 2002;42(4):368-374.

14. Ode M, Suzuki T, Kim SG, Kim WT. Phase-field model for solidification of Fe-C alloys. *Science and Technology of Advanced Materials*. 2000;1:43-49.
15. Meza ES, Bertelli F, Goulart PR, Cheung N, Garcia A. The effect of the growth rate on microsegregation: Experimental investigation in hypoeutectic Al-Fe and Al-Cu alloys directionally solidified. *Journal of Alloys and Compounds*. 2013;561:193-200.
16. Oguchi K, Suzuki T. Phase-Field Simulation of Free Dendrite Growth of Aluminum-4.5 mass% Copper Alloy. *Materials Transactions*. 2007;48(9):2280-2284.
17. Wesner E, Choudhury A, August A, Berghoff M, Nestler B. A phase-field study of large-scale dendrite fragmentation in Al-Cu. *Journal of Crystal Growth*. 2012;359:107-121.
18. Choudhury A, Reuther K, Wesner E, August A, Nestler B, Rettenmayr M. Comparison of phase-field and cellular automaton models for dendritic solidification in Al-Cu alloy. *Computational Materials Science*. 2012;55:263-268.
19. Boettinger WJ, Warren JA, Beckermann C, Karma A. Phase-Field Simulation of Solidification. *Annual Review of Materials Research*. 2002;32:163-194.
20. Qin RS, Bhadeshia HK. Phase-field method. *Materials Science and Technology*. 2010;26(7):803-811.
21. Ode M, Kim SG, Kim WT, Suzuki T. Numerical Prediction of The Secondary Arm Spacing Using a Phase-Field Model. *ISIJ International*. 2001;41(4):345-349.
22. Kurum EC, Dong HB, Hunt JD. Microsegregation in Al-Cu Alloys. *Metallurgical and Materials Transactions A*. 2005;36(11):3103-3110.